Supporting Information

Switchable plasmonic metasurfaces with high chromaticity containing only abundant metals.

Kunli Xiong,[1] Daniel Tordera,[2] Gustav Emilsson,[1] Oliver Olsson,[3] Ulrika Linderhed,[4] Magnus P. Jonsson[2] and Andreas B. Dahlin.[1]*

1 Dept. of Chemistry and Chemical Engineering, Chalmers University of Technology, 41296 Göteborg, Sweden.

2 Linköping University, Dept. of Science and Technology, Laboratory for Organic Electronics, 60174 Norrköping, Sweden.

3 rdot AB (559092-9831), Stena Center 1, 41292 Göteborg, Sweden.

4 RISE Acreo, Box 787, 60117 Norrköping, Sweden.

*** Corresponding author: adahlin@chalmers.se**

Materials and methods

Nanofabrication: Glass slides were cleaned by 50 W oxygen plasma for 10 min. PET supports were cleaned by sonication in ethanol for 5 min. All depositions were achieved with automated electron beam evaporation (Lesker PVD225). Colloidal lithography was performed on freshly deposited Al_2O_3 as described previously[1, 2] using commercial polystyrene-sulphate colloids (Microparticles GmbH). The characteristic spacing of the short-range order was determined by image analysis as in previous work.[1-3] To create microscale pixels, patterns were written by a laser writer (Heidelberg Instruments DWL 2000). The photoresist (LOR3A) was spin coated at 4000 rpm and baked on a hotplate at 180 °C for 5 min. A second layer of S1813 was spin coated at 4000 rpm and baked on a hotplate at 120 °C for 2 min. Pixels for one primary color were then patterned by the 60 mW laser beam after which the sample was developed in developer MF-318 for 50 s. The rest of the nanostructure was then fabricated and the process was repeated two times for each primary color.

Spectroscopy: The dark spectrum of the spectrometer (B&WTek CypherX) was recorded with the illumination off and subtracted from subsequent acquisitions. The light source was a 100 W halogen lamp (Newport). The reference intensity for reflection mode was measured by a commercial Ag mirror (Thorlabs BBE02-E02). Various air objectives with different NA were used in a customized setup where the reflected light was coupled to an optical fiber. Extinction spectroscopy on Cu nanohole arrays was performed as described previously.[2] Note that reflectivity is the ratio of measured intensity and reference intensity, while extinction is the natural logarithm of the inverse of this ratio.

Pictures: Photos were taken with an iPhone 6 using standard settings, no flash and high dynamic range off. No regions of the photos have been manipulated. In all images that compare “color on”

and “color off” states, image settings such as brightness and contrast are identical. Dark field images were collected by epi-illumination in air with a 50× NA 0.8 objective. Microscopy images were captured by a Zeiss Axiocam506 camera.

Image processing: The masks used for laser lithography were generated using MATLAB and the GDSII toolbox. Each pixel in the original image was transferred into mask pixels consisting of three subpixels each. The width of each subpixel was set to 30 μm and the spacing between them to 5 μm (no spacing between pixels). The color values for each pixel in the original image was converted into the corresponding subpixel height using the expression round(cval/255×hmax) where hmax was set to 100 μm and cval is the value obtained from the corresponding color channel (0-255 for R, G or B) of the original image.

Screen printing: 550 nm thick poly(3,4-ethylenedioxythiophene) polystyrene sulfonate (PEDOT:PSS, Heraeus Clevios SV4) layers were screen-printed on top of the MIN metasurfaces. A DEK Horizon 03iX printer was used with a 61-64 mesh (61 threads/inch, 64 μm thread diameter). The PEDOT:PSS was subsequently annealed at 130 °C for 4 min by using a Natgraph Air Force UV Combination Dryer.

Reflectivity from metasurfaces with other Cu nanohole arrays

Examples of reflectivity from metasurfaces with other nanohole arrays are shown in Fig. S1. For blue-green samples (~110 nm Al_2O_3), the reflectivity in the red region is higher for the nanohole arrays with D = 107 nm or D = 198 nm (c.f. Fig. 2 in main text). When there are no holes in Cu the reflectivity in the red goes up a lot and the samples become magenta. The red samples (~75 nm Al_2O_3) are always red regardless of nanohole array, but there is never a significant improvement compared to having no holes. For all samples with h = 30 nm the reflectivity increases in the spectral regions outside of the resonant color, which also leads to poorer chromaticity.

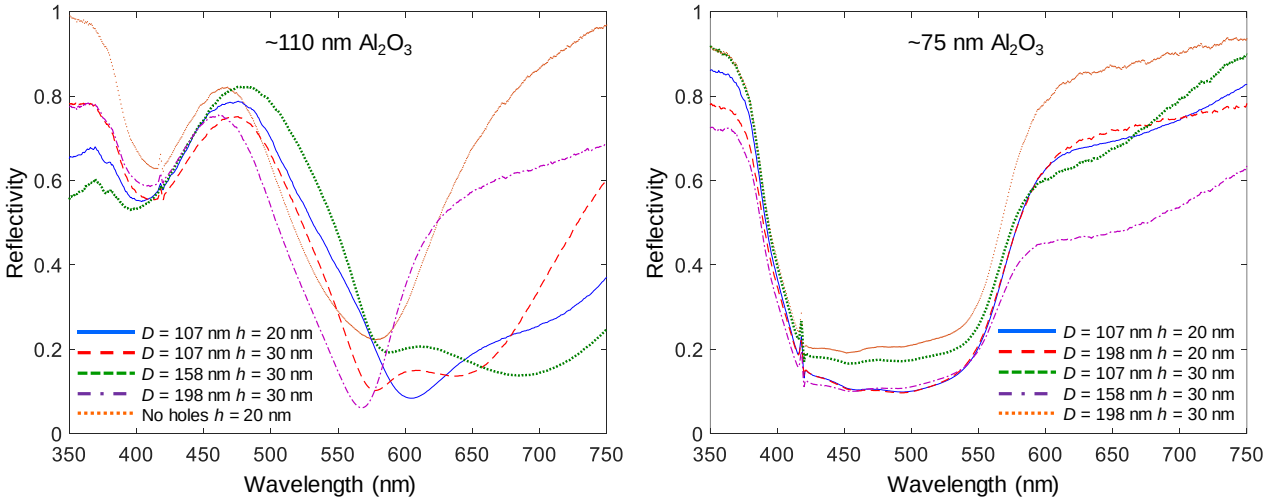

Figure S1. Examples of non-optimal (in terms of primary colors) reflectivity from metasurfaces with other dimensions chosen for the MIN nanostructure. In the left plot the Al_2O_3 thickness is such that the resonant reflection lies in the blue-green region, while the reflection is red in the right plot. Different nanoholes are used as described by the legends.

Dispersion relations for surface plasmons

We first calculated the dispersion relation of the bonding surface plasmon mode[3] in a 20 nm Cu film on glass (n = 1.5) with 20 nm Al_2O_3 on top (n = 1.7) and exposed to air (n = 1). The bonding mode was identified by the asymmetric field distribution (symmetric charge distribution) across the film, which is also obtained with this method.[1] Based on image analysis of the short-range ordered apertures the effective periodicities of the arrays were set to 210, 310 and 390 nm for 107, 158 and 198 nm colloids respectively. Fig. S2 shows the result for a 20 or 30 nm Cu film and the predicted (first order) resonance occurring when the periodicity of the array matches the mode wavelength.

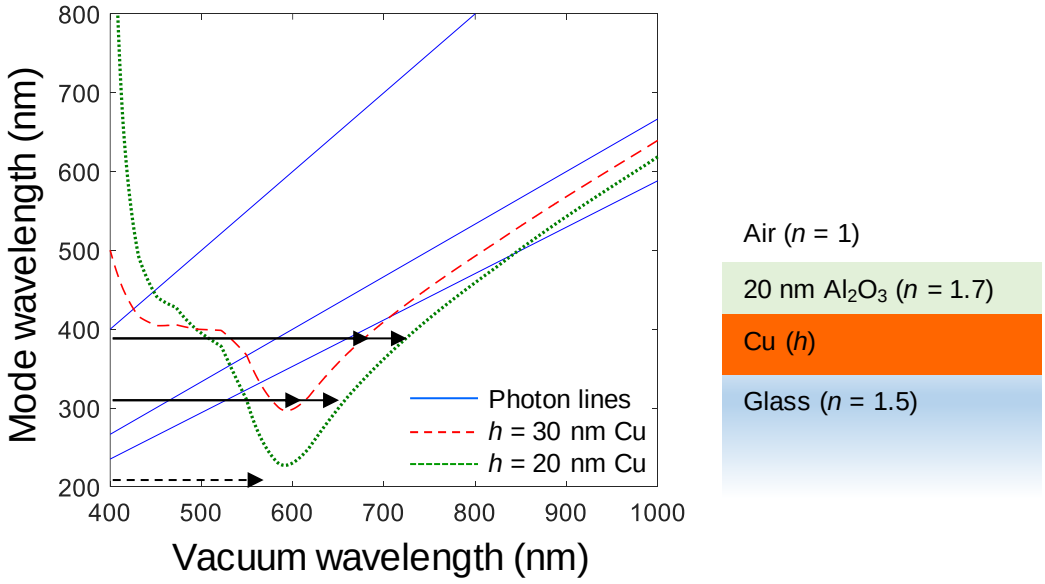

Figure S2. Calculated dispersion relations for bonding surface plasmon mode in finite Cu films on glass with an additional Al_2O_3 coating. The arrows indicate the predicted resonances based on the quasi-periodicity of the experimental short-range ordered nanohole arrays.

The calculated resonance wavelengths were compared with the experimental (Fig. 1 in main text) as summarized in Table S1.

Array	Predicted resonance (nm)	Measured resonance (nm)	Error (nm)
D107h20	Not predicted	667	?
D158h20	657	688	-31
D198h20	726	744	-18
D107h30	Not predicted	605	?
D158h30	614	626	-12
D198h30	680	659	+21

Table S1: Predicted and measured resonance wavelengths (extinction peak position) for nanohole arrays in a single Cu film on glass.

Overall, the predicted values are in fair agreement with experimental data and illustrate the effect of increased Cu thickness and spacing between the holes (effective periodicity). As has been shown previously there is an error on the order of tens of nm because the presence of holes in the metal film is not accounted for,[3] i.e. the metal film has another effective permittivity than the bulk material. For short wavelengths the dispersion relation behaves anomalously due to Cu absorption and a solution cannot be found because the permittivity of the metal film is not entirely correct. Retardation is still accounted for in these calculations[1] i.e. the solution is an imaginary wavevector which thus also contains the predicted propagation length of the wave. For these Cu films the propagation length was on the order of 1 μm in the red and essentially zero for vacuum wavelength below ~600 nm as expected due to Cu absorption.

The predicted resonances in the MIN system with 20 nm Cu are shown in Fig. S3 for different values of Al_2O_3 thickness. As expected, the resonance blueshifts as the thickness of Al_2O_3 is reduced (for the same mode wavelength) due to coupling to the underlying Al film, illustrating the color tuning by surface plasmons. Assuming the predicted resonance has roughly the same error

as for the calculation on only the Cu film layer (Fig. S2), the predicted values indeed lie in the yellow-red region 550-600 nm. Thus the surface plasmon theory is consistent with the colors observed under dark-field illumination (Fig. 3A in main text).

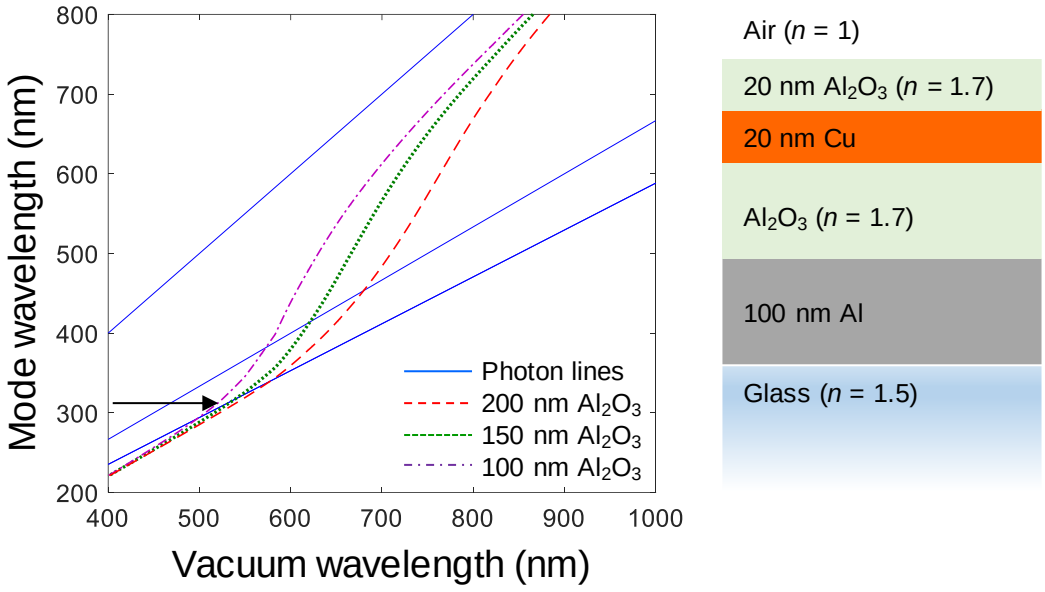

Figure S3. Calculated dispersion relations for the excited mode in a system with Al and Cu films with different values for the Al_2O_3 thickness. The Cu thickness is 20 nm in all cases. The arrow indicates the predicted resonance for a mode wavelength corresponding to samples prepared with 158 nm colloids.

Simulation results

The reflectivity of the MIN metasurfaces was modelled in COMSOL Multiphysics 5.0 Wave Optics frequency domain. An incident plane wave illuminated the sample from top. The permittivity of each material was the same as in the dispersion relation calculations. The short-range ordered nanohole array was represented by a square lattice with a periodicity equal to the experimental nearest-neighbor distance (310 nm for D = 158 nm). The Cu film was h = 20 nm with 20 nm Al_2O_3 on top. As we have shown in previous work, representing the short-range ordering in this manner reproduces the experimental far field spectra well.[1-3] We also simulated the transmission through only the nanohole arrays in Cu, which gave equally good agreement with experiments (Fig. 1 in main text) except that the resonance peak was sharpened as expected.[3]

The simulations show that the reflectivity is reduced in the red region when nanoholes are introduced in the Cu film, as observed experimentally. In addition, the holes do not give a significant change in the reflectivity peak from the cavity mode for blue and green, again in agreement with experiments. However, the reflectivity decrease in the red region due to the holes is not as high as in the experiments, which can be attributed to the long-range ordering of the apertures in simulations. For the experimental short-range ordered samples, scattering of light is a very strong decay channel for the plasmons.[4]

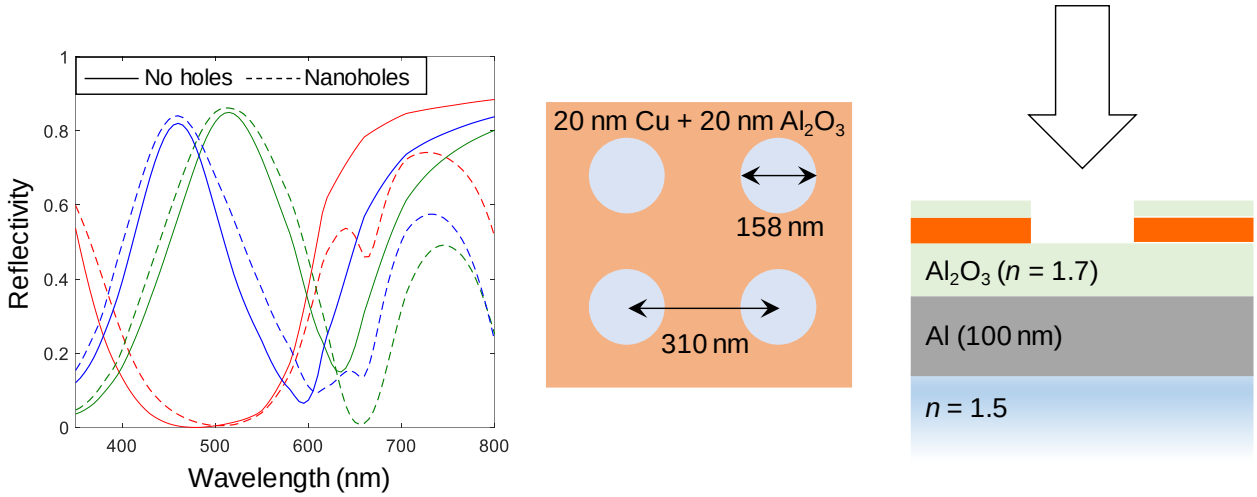

Figure S4. Simulated reflectivity at zero incidence from the metasurfaces with and without nanoholes in Cu. The arrays were represented by a square lattice with periodicity of 310 nm. The Al_2O_3 thickness is 75, 103 and 115 nm for red, blue and green as in the real samples. Other parameters are as for the dispersion relation calculations.

Current response when switching

The current trace when switching the conductive polymer film (±1 V) is shown in Fig. S5. The integrated current from one cycle with background subtracted gave a switching charge density of 5.7 mC/cm^2. The charge transfer is consistent with a thickness of ~500 nm considering the typical density of polymer films and that not all PEDOT monomers switch (and no PSS monomers at all).

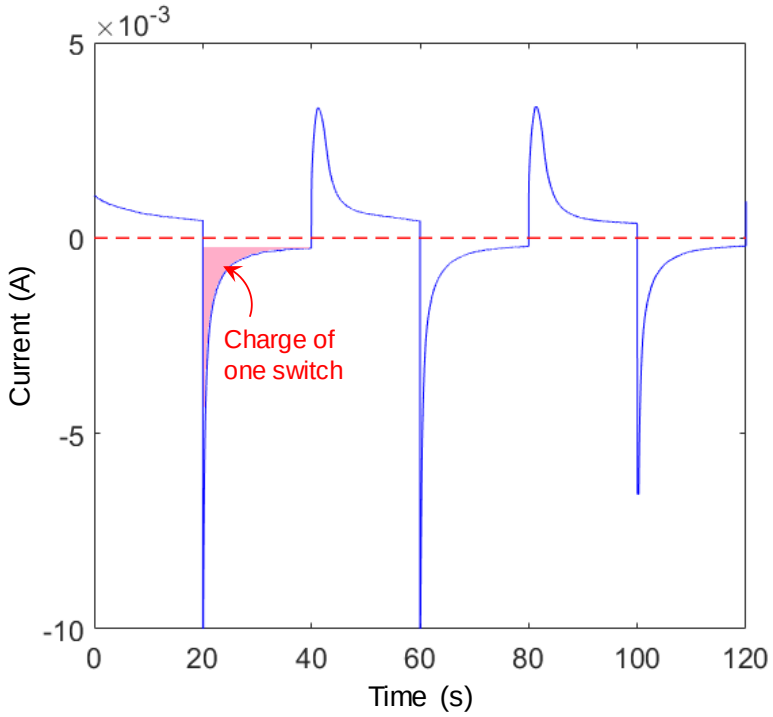

Figure S5. Current monitored when switching PEDOT:PSS (Fig. 4 in main text). The electrode area was 1.77 cm^2. Note that these data look the same regardless of metasurface color since the polymer layer was always the same. The voltage was square wave as for the data in main text.

Angle and polarization dependence

The angle dependence was first characterized by measuring the reflectivity with different objectives in air in order to vary the incident angle range (not one specific angle). Example of data for red, green and blue metasurfaces is shown in Fig. S6. The spectral changes are comparable to the sample to sample variation in magnitude. Based on the NA values of the objectives this strongly suggests the angle dependence of the reflected color is very small up to at least 40°.

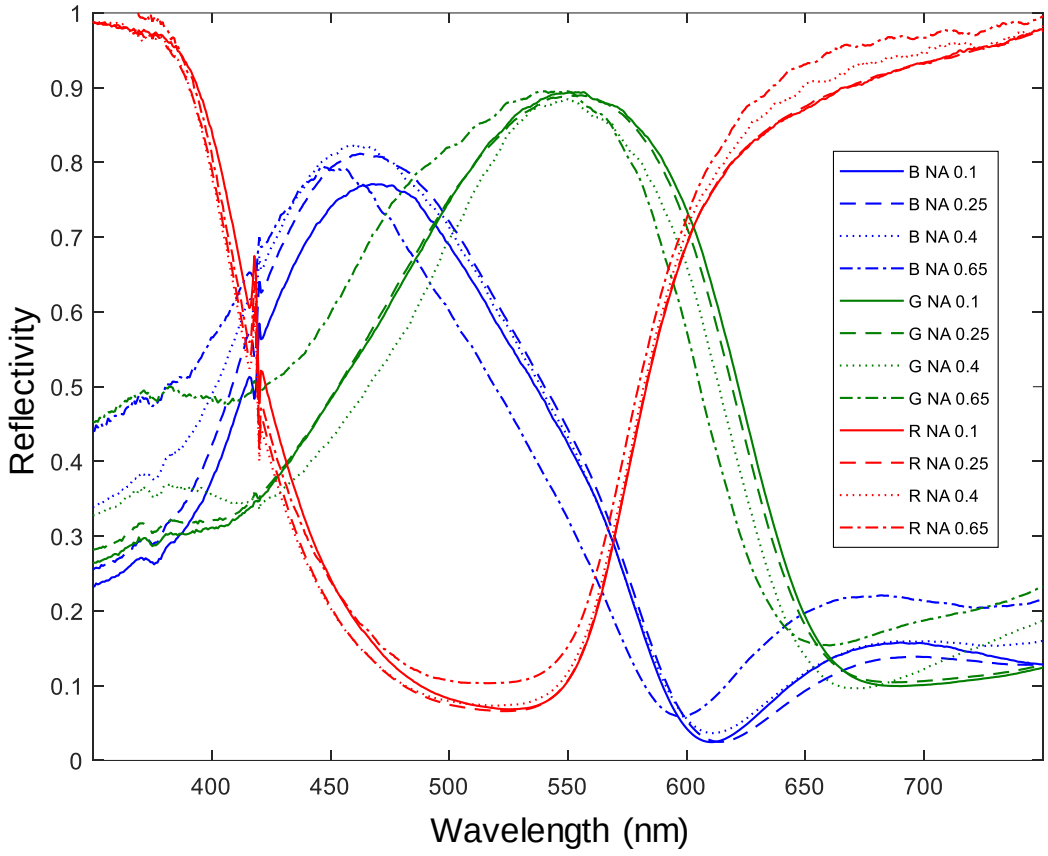

Figure S6. Reflectivity of metasurfaces measured in air with different microscope objectives. (The angular illumination/collection range is up to 6° for NA 0.1 and up to 41° for NA 0.65.)

Further, we used a spectroscopic ellipsometer (Wollam M2000) to measure the angular and polarization dependence of the specular reflection at angles of 45° or more. Fig. S7 shows an example of data from a green metasurface. The results show that at such high angles the colors do

start to change as expected from the cavity mode. The plasmonic activity in the red region keeps the reflectivity lowered, although not as low as angles close to normal incidence (c.f. Fig. S6). Further, the plasmon excitation appears not strongly dependent on polarization as expected.[5]

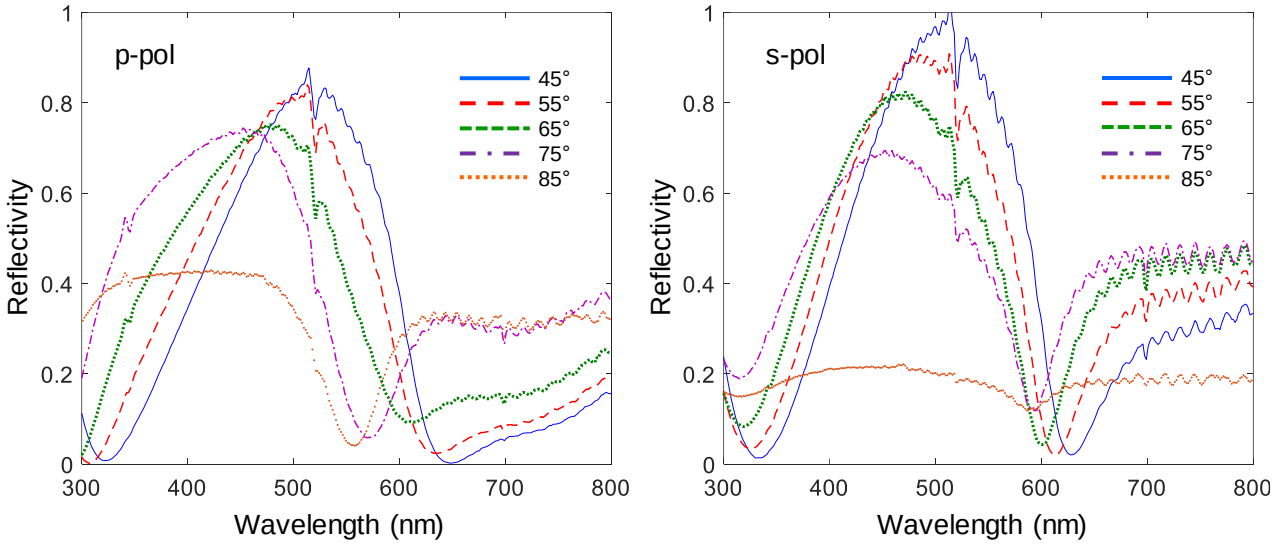

Figure S7. Reflectivity of a green metasurface at different specific angles of incidence for p (left) or s (right) polarization. Note that no scattered light is collected in these measurements.

To verify that the reflectivity changes with angle and polarization from the cavity mode are as expected we also performed Fresnel calculations on the thin film system without nanoholes (Fig. S8). The Al_2O_3 thickness was set to 140 nm. Again, the reflectivity in the red region is higher since there is no coupling to surface plasmons and hence the chromaticity is poorer. The shift in the peak from the cavity mode with angle of incidence is in good agreement with experiments on metasurfaces (c.f. Fig. S7).

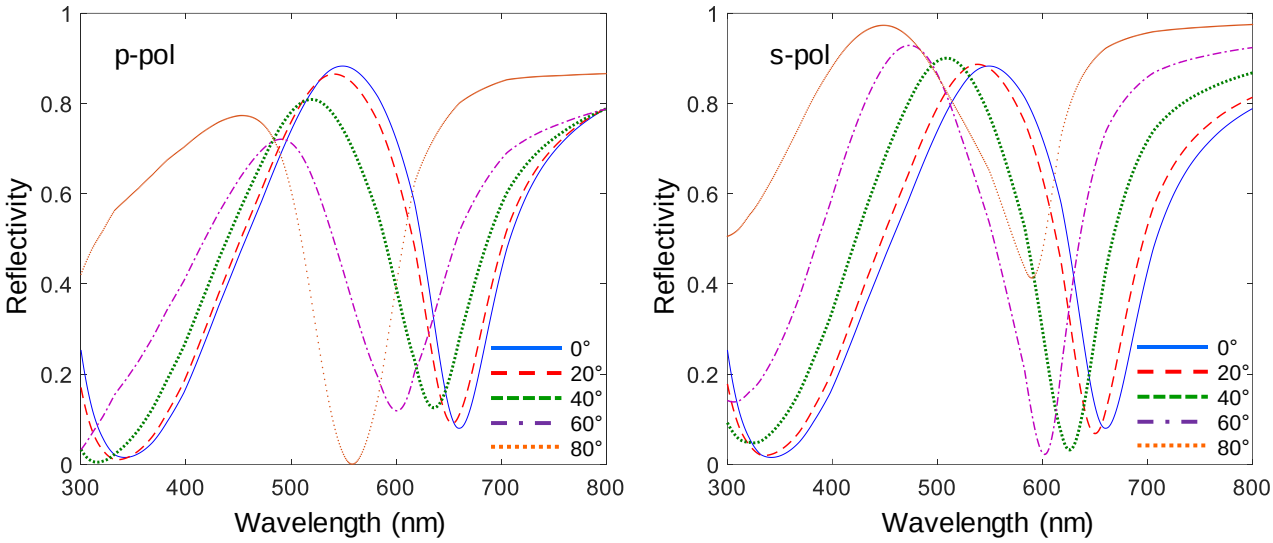

Figure S8. Fresnel models of reflectivity from the thin film system (no nanoholes). The permittivities were set as in the other calculations and the Al_2O_3 thickness was 140 nm.

Metasurfaces prepared with only Al

When using only Al to produce the MIN metasurfaces, i.e. when Cu is replaced by Al for the nanohole array, the colors range is much more limited. A photo of the best "Al only" sample we could produce is shown in Fig. S9. It is obvious that regardless of Al_2O_3 thickness the primary colors red, green and blue are not as clear as when using Cu (main text). Overall the visual appearance is very similar to previous work presenting coloration with Al nanostructures.[6-8]

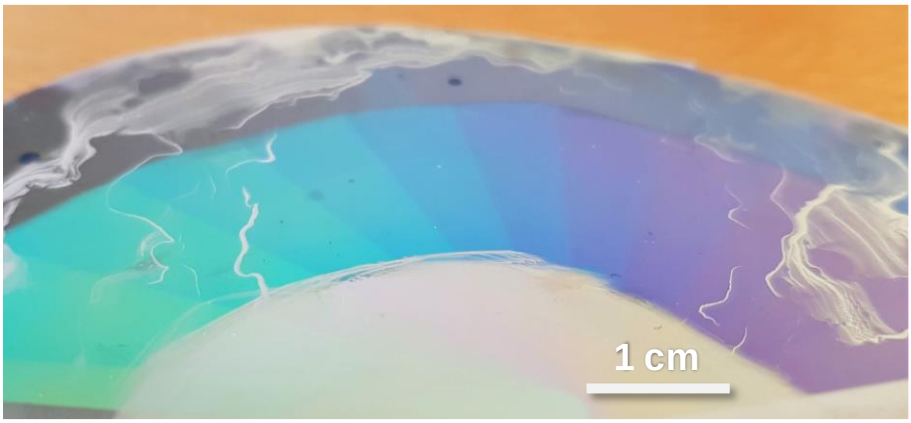

Figure S9. Color range obtained by using Al also for the nanohole array. The Al_2O_3 thickness ranges from 50 nm (purple) to 105 nm (cyan) in steps of 5 nm.

Regarding optimal colors and contrast

A brief proof that there is an optimal thickness for the polymer film is given here. We assume that there are no significant interference effects in the polymer film, which is reasonable since its refractive index normally is very similar to the electrolyte.[9] The incident intensity is I_0 and the reflected intensity is I. We are looking for the reflectivity $R = I/I_0$. The underlying metasurface reflectivity is R_0. The light passes through the polymer layer of thickness d twice. By using a Lambert-Beer type expression the transmitted intensity follows a logarithmic dependence:

$$R(\lambda) = R_0(\lambda)\exp(-2C\sigma(\lambda)d) \qquad \text{(S1)}$$

Here C represents the concentration of optically active monomers in the polymer film, where each has a cross section σ. The expression illustrates that the reflectivity depends on both the metasurface reflectivity and the absorption spectrum of the polymer. Ideally one should combine each colored metasurface with a polymer composition that leads to absorption of the complementary colors.

When the polymer switches between absorption state σ_1 and σ_2 the corresponding reflectivity change is:

$$R_2 - R_1 = R_0\left[\exp(-2C\sigma_2 d) - \exp(-2C\sigma_1 d)\right] \qquad \text{(S2)}$$

To optimize the difference in reflectivity one should thus also consider the polymer thickness.[10] Clearly, since the contrast is proportional to the difference between two exponentially decaying functions there must be an optimum value for d (although different depending on wavelength). Deriving and solving for this value gives:

$$d_{\text{opt}} = \frac{\log\left(\frac{\sigma_2}{\sigma_1}\right)}{2C\left[\sigma_2 - \sigma_1\right]} \qquad \text{(S3)}$$

Kuggen building source file

The image file is included as online material. The image was downloaded from:

https://mabrycampbell.wordpress.com/2014/12/04/the-kuggen-in-gothenburg-sweden/

The resolution was reduced to 512×341 to make the full image fit well on the wafers given the defined pixel widths. The same lower resolution version was used for inkjet printing. The Copyright belongs to Mabry Campbell Photography. Permission to use the image “The Kuggen Connection” for this study was obtained from the copyright holder.

References (also cited in main text)

1. Dahlin, A. B.; Mapar, M.; Xiong, K. L.; Mazzotta, F.; Hook, F.; Sannomiya, T. *Adv. Opt. Mater.* **2014,** 2, 556-564.

2. Xiong, K.; Emilsson, G.; Dahlin, A. B. *Analyst* **2016,** 141, 3803-3810.

3. Sannomiya, T.; Scholder, O.; Jefimovs, K.; Hafner, C.; Dahlin, A. B. *Small* **2011,** 7, 1653-1663.

4. Prikulis, J.; Hanarp, P.; Olofsson, L.; Sutherland, D.; Kall, M. *Nano Lett.* **2004,** 4, 1003-1007.

5. Reilly, T. H.; Tenent, R. C.; Barnes, T. M.; Rowlen, K. L.; van de Lagemaat, J. *ACS Nano* **2010,** 4, 615-624.

6. Clausen, J. S.; Hojlund-Nielsen, E.; Christiansen, A. B.; Yazdi, S.; Grajower, M.; Taha, H.; Levy, U.; Kristensen, A.; Mortensen, N. A. *Nano Lett.* **2014,** 14, 4499-4504.

7. James, T. D.; Mulvaney, P.; Roberts, A. *Nano Lett.* **2016,** 16, 3817-3823.

8. Tan, S. J.; Zhang, L.; Zhu, D.; Goh, X. M.; Wang, Y. M.; Kumar, K.; Qiu, C.-W.; Yang, J. K. W. *Nano Lett.* **2014,** 14, 4023-4029.

9. Xiong, K.; Emilsson, G.; Maziz, A.; Yang, X.; Shao, L.; Jager, E. W. H.; Dahlin, A. B. *Adv. Mater.* **2016,** 28, 9956-9960.

10. Malti, A.; Brooke, R.; Liu, X.; Zhao, D.; Andersson Ersman, P.; Fahlman, M.; Jonsson, M. P.; Berggren, M.; Crispin, X. *J. Mater. Chem. C* **2016**, 4, 9680-9686.